1.13

ELASTIC INSTABILITY OF CONICAL SHELLS UNDER COMBINED LOADING

by P. P. Radkowski

Avco Research and Advanced Development Division

SUMMARY

1. Criteria are presented for the elastic instability of thin single and multilayer conical and cylindrical shells under combined axial load and external pressure. These criteria,used in design analysis, are based on theoretical results and the correlation of these results with readily available experimental data.

2. A summary is included of the studies at Avco RAD of shells under static or dynamic loads.

INTRODUCTION

In designing vehicles for space and/or re-entry environments, many interrelated parameters must be considered. Overall optimization of a design can best be achieved by studies showing the tradeoff between the various parameters which are chosen. One of the most critical problems in achieving this optimization is to obtain more reliable information on the instability of conical shells under combined lateral pressure and axial loading.

The analytical results of reference 1 have been extended and correlated with readily available experimental data; a relatively simple formula may now be used for an elastic instability analysis of conical and cylindrical shells. This report shows that further analysis is required for correlation and interpretation of analytical and experimental results for design purposes.

SYMBOLS

B = effective extensional modulus,

D = effective bending modulus,

E = Young's modulus,

K = $\dfrac{(1-\nu^2)\ell^2 B}{\pi^2 k^2 D(\bar{k}_1 - 1)^4}$,

L = total axial load (positive in compression),

$\bar{M}$ = $\dfrac{L\ell}{2\pi^2 k \; D(\bar{k}_1 - 1)^2 \sin^2\alpha}$

P = $-\dfrac{\ell^2 B k_2 p_{cr}}{\pi^2 D(\bar{k}_1 - 1)}$,

a = largest base radius,

h = thickness of shell,

k = $\dfrac{\pi a(1-\beta/2)}{\ell \sin\alpha}$,

$\bar{k}_1$ = $\dfrac{\beta(1-(2/3)\beta)}{2(1-\beta/2)^2}$,

k_2 = $\dfrac{k\ell}{\pi B}$,

ℓ = slant length,

p_{cr} = critical lateral pressure,

α = base angle

β = $(\ell/a)\cos\alpha$,

ρ = $\dfrac{a(1-\beta/2)}{\sin\alpha}$ = average radius of curvature, and

ν = Poisson's ratio.

DISCUSSION

L
3
1
0
9

Theoretical Buckling Criteria

The equation, derived in reference 2,

$$\frac{P}{|P_{int}|_T} = -\frac{2}{13}\left(\frac{\bar{M}}{|\bar{M}_{int}|_T}\right)^2 + \frac{5}{6}\left(\frac{\bar{M}}{|M_{int}|_T}\right) + 1 \tag{1}$$

is a relation approximating the theoretical buckling criteria for single and multilayer conical and cylindrical shells subjected to axial load and lateral pressure. This relation is a reasonable approximation to the theoretical relation for $10 < \sqrt{K} < 10,000$. Here,

$$|\bar{M}_{int}|_T = 2\sqrt{K} \quad \text{and} \quad |P_{int}|_T = \frac{4}{3}\left[1 + (3K)^{1/4}\right] \tag{2}$$

are the theoretical intercepts of the curve with the $\bar{M}$ and P axes respectively. For design purposes, these intercept relations will be replaced by relations based upon theoretical and experimental results.

Experimental results and correlation with theoretical results. - The experimental results are divided into two categories, i. e., hydrostatic and lateral pressure, and axial load. The data is then correlated with theoretical results for an interaction curve for combined loading. Many test results exist for either axial load or hydrostatic loading of cylinders, but only a limited number of test results exist for combined loading.

Hydrostatic loading. - Figure 1 shows only a small portion of the available experimental data and the scatter is considerable. Several years ago a systematic evaluation of the available data was initiated. Some of the conclusions are shown in figure 2; a more extensive set of results with the tabulation of readily available experimental data are given in reference 3. Here, we consider the base angle $\alpha = 30$ degrees and plot $p_{cr}\ 10^6/E$ versus ℓ/a for various values of h/a. A plot of p_{cr}/E versus α is given in figure 3 for a fixed value of h/a and ℓ/a.

It is extremely difficult to evaluate all of the experimental results, because some of the experimenters chose the buckling pressure when the first buckle or lobe appeared, while others chose the pressure when all the lobes appeared. The ideal case, as assumed, would be when all lobes appeared simultaneously at one pressure. Some of the tests observed and listed in reference 3 showed that when the first lobe appeared, e. g., at pressure p_1 the pressure dropped, and as the pressure was increased again the remaining lobes appeared but at a pressure less than p_1. However, in other tests listed in reference 4 the reverse was the case, i. e., after the first lobe appeared the pressure dropped, and as the pressure was increased again the remaining lobes appeared but at a pressure greater than p_1. Probably, the appearance of the first lobe distorted the remaining structure so as to render the resulting configuration weaker in one case and stronger in the other. Except for reference 4, all of the data reported used the pressure when the first lobe appeared as the critical pressure. The experimental data reveals some scatter as expected. This scatter is probably due to test techniques, physical properties of the material, imperfection and variation in geometry, different edge restraints, and possible nonuniform edge restraints.

To determine the data used in plotting the banks of curves, the theoretical curves were used as a basis of study and then modified to conform to the experimental results listed in reference 3. The modifications were accomplished in the horizontal portion of the typical curve given in figure 2. In almost every case the horizontal portion remained horizontal for h/a of the order of 10^{-3}, and as h/a increased towards 10^{-2} the slope increased negatively. Where the curve is nearly horizontal the theoretical and the limited experimental results agreed remarkably well. However, in the region where the horizontal portion of the curve was modified and h/a was of the order of 10^{-2}, the difference between the experiments and the predicted theoretical values could be as high as a factor of two for a nontruncated cone, e.g., when $\alpha = 70$ degrees and $h/a = 10.6 \times 10^{-3}$. Although, in general, relatively good correlation exists between the limited number of experimental and theoretical results, the designer should use his own discretion.

In figure 3, p_{cr}, pressure versus α is plotted. A maximum appears for a base angle between 60 to 70 degrees. Only 18 experimental data points for α less than 30 degrees and various ℓ/a and h/a were available at this time and the curve for this range might have to be modified.

To summarize the hydrostatic loading analysis, very little experimental data exists for (1) $\alpha<30$ degrees, (2) $\ell/a<1$ for all angles, (3) h/a of the order 5×10^{-3}, and (4) multilayer cones. Interestingly, the critical buckling pressure could vary by a factor of 2 or more for a variation of α within 10 degrees.

L 3 1 0 9

Axial load. - The data for axial load, shown in figure 4, is somewhat scattered as it was for the lateral pressure case; this scattering could be due to the factors similar to those for the hydrostatic case. Data from reference 4 is somewhat higher than the other results shown in figure 4, from references 5 and 6. Probably, this is due to the fact that the load which gave the first buckle was considered the critical load in most experiments, while reference 4 gives the load which gave all the buckles as the critical load. From a design viewpoint the critical load which gives all of the buckles may be considered, i. e., where the buckles do not affect the load carrying capacity of the structure. However, in re-entry vehicles a single buckle, or lobe, may cause the thermal protection system to fail and then the whole system fails. Consequently, the curve beneath all of the experimental data would normally be used for design studies of re-entry vehicles.

The experimental data for axial loading should be analyzed to determine the effect of angle, length, thickness, radius, and materials (among other factors) on the critical load applied to conical and cylindrical shells. Studies of this type have been initiated and results should be published as soon as they are available.

A criterion for combined loading. - In certain cases of designing conical shells, equation 1 is not sufficient. In general, equation 1 is an upper bound for the combined loading case; a lower bound should be used. Several methods of determining a lower bound suggest themselves. To determine a lower bound for P_{int} (lateral pressure only), refer to figure 1. Curve C is plotted through the two lowest experimental curves, and for most purposes, is a reasonable value for the lower bound. The equation for curve C can be written as,

$$P^4 = K \tag{3}$$

Consequently, the new P_{int} for equation 1 can be

$$P_{int} = 4\sqrt{K} \tag{4}$$

As an alternative, the results of reference 3 may be used, typified by figure 2, for determining a more refined P_{int}.

For the lower bound of $\bar{M}_{int}$ (axial load only), one proceeds as in determining P_{int}, which is given in equation 4. Here,

$$|\bar{M}_{int}| = \frac{5}{8}\sqrt{K}, \frac{\rho}{h} \leq 450 ,$$

$$|\bar{M}_{int}| = \frac{1}{2}\sqrt{K} \quad 450 < \frac{\rho}{h} \leq 600 ,$$

$$|\bar{M}_{int}| = \sqrt{\frac{2}{5}}\,K , \quad 600 \leq 900$$

$$|\bar{M}_{int}| = K^{2/5} , \quad 900 < \frac{\rho}{h} \leq 2000$$

$$|\bar{M}_{int}| = \frac{5}{3}\,K^{1/3} \quad 2000 < \frac{\rho}{h} \leq 3000 \tag{5}$$

The expressions in equation 5 are comparable to those of reference 6.

Figure 5 illustrates the use of equation 3. Experimental Avco RAD* combined loading data are plotted, and their relationship to the curve of equation 1 is shown. The choice of $\bar{M}_{int}$ and P_{int} will depend upon geometrical considerations (in this case, see equation 5 for $\bar{M}_{int}$, and reference 3 for P_{int}. It is apparent that further refinements are necessary for $\bar{M}_{int}$

Summary of studies on instability due to static loading. - The instability of isotropic shells of revolution has been completed and will be presented in a forthcoming report, reference 7. This report gives a simplified energy relation based on Donnell-type assumptions. A set

*These experiments were conducted by R. H. Homewood and are as yet unpublished of displacement functions are used which are slightly more general than those used for noncylindrical shells. The instability of toroidal shells subject to internal or external loading is presented as a relatively simple formula; an energy solution for a truncated spherical shell subject to compressive loading is also presented. Very few experimental or analytical results are available for shells other than the cone, cylinder and shallow sphere.

Very little experimental data appear to be available for any type of multilayer shell of revolution subject to compressive loading.

Several experiments are being carried out at Avco RAD for a pressure distribution varying linearly over the slant length of a conical shell.

Summary of studies on instability due to a pressure pulse. - For several years studies have been made of the dynamic response of shell structures and materials subjected to a pressure pulse. This problem could be characterized (1) by shell-fluid interaction, such as water entry of a shell-like structure, and (2) by applying a sheet explosive over a portion of a cylinder with results as illustrated in figures 6 and 7. This application of a sheet explosive over a portion of a cylinder is characterized by very high pressures for very short times, which presents a dynamic boundary condition not often treated in recently published literature. The problem of the behavior of cylindrical and spherical shells under such conditions have been approached from two extremes; ideal elastic buckling and ideal rigid-plastic collapse (reference 8). The work on elastic buckling of cylinder and sphere is for a pressure time history. The analysis of a shallow sphere is presented at this symposium by Professor B. Budiansky.

As in the case of buckling of shells under static loading, considerably more analytical and experimental work is necessary for a truly definitive understanding of the problem of dynamic response of shell-like structures. Experimental and analytical investigations have been undertaken at several universities and by private industry. These efforts should help to provide the means of corroborating the present theoretical understanding and the basis for additional analytical and experimental work.

REFERENCES

1. Radkowski, P. P.: Buckling of Single- and Multi-Layer Conical Cylindrical Shells with Rotationally Symmetric Stresses. Proceedings of the Third U. S. National Congress of Applied Mechanics, ASME, June 11-14, 1958.

2. Radkowski, P. P.: Buckling of Single- and Multi-layer Conical and Cylindrical Shells Subjected to Axial Loads and Lateral Pressure. Avco RAD TR-61-36, Dec. 1961.

3. Radkowski, P. P.: Correlation of Analytical and Experimental Results of the Instability of Conical Shells under Hydrostatic Pressure. Avco RAD (in preparation).

4. Weingarten, V. I., Morgan, E. J., and Seide, P.: Development of Design Criteria for Elastic Stability of Thin Shell Structures. STL/TR 60-0000-19425, Dec. 31, 1960.

5. Lockman, L. and Penzien, J.: Buckling of Circular Cones under Axial Compression. Jour. Applied Mech., vol 27, Sept. 1960, pp. 458-460.

6. Batdorf, S. B., Schildcrout, M., and Stein, M.: Critical Stress of Thin-walled Cylinders in Axial Compression. NACA Report 887, 1947.

7. Radkowski, P. P.: Buckling of Thin Single- and Multi-Layer Shells of Revolution with Rotationally Symmetric Stresses. Avco RAD TR-62-1, Dec. 1961.

8. Radkowski, P. P., Humphreys, J. S., Payton, R. G., Bodner, S. R., and Budiansky, B.: Studies on the Application of X-ray as a Lethal Mechanism on Decoy Discrimination Technique (vol. 2) Studies on the Dynamic Response of Shell Structures and Materials to a Pressure Pulse. Avco RAD TR 61-31, July 1961.

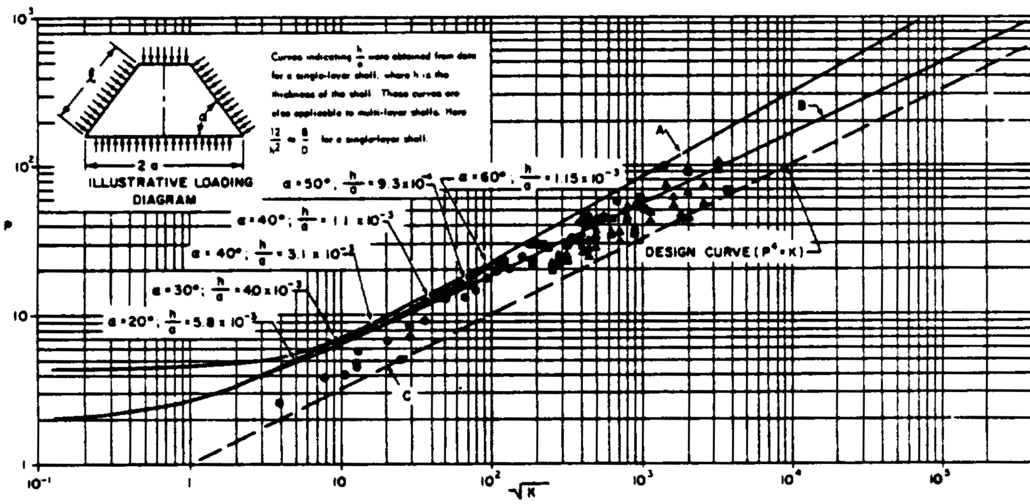

59-458

Figure 1. - Critical pressure curves for thin single- and multi-layer conical and cylindrical shells.

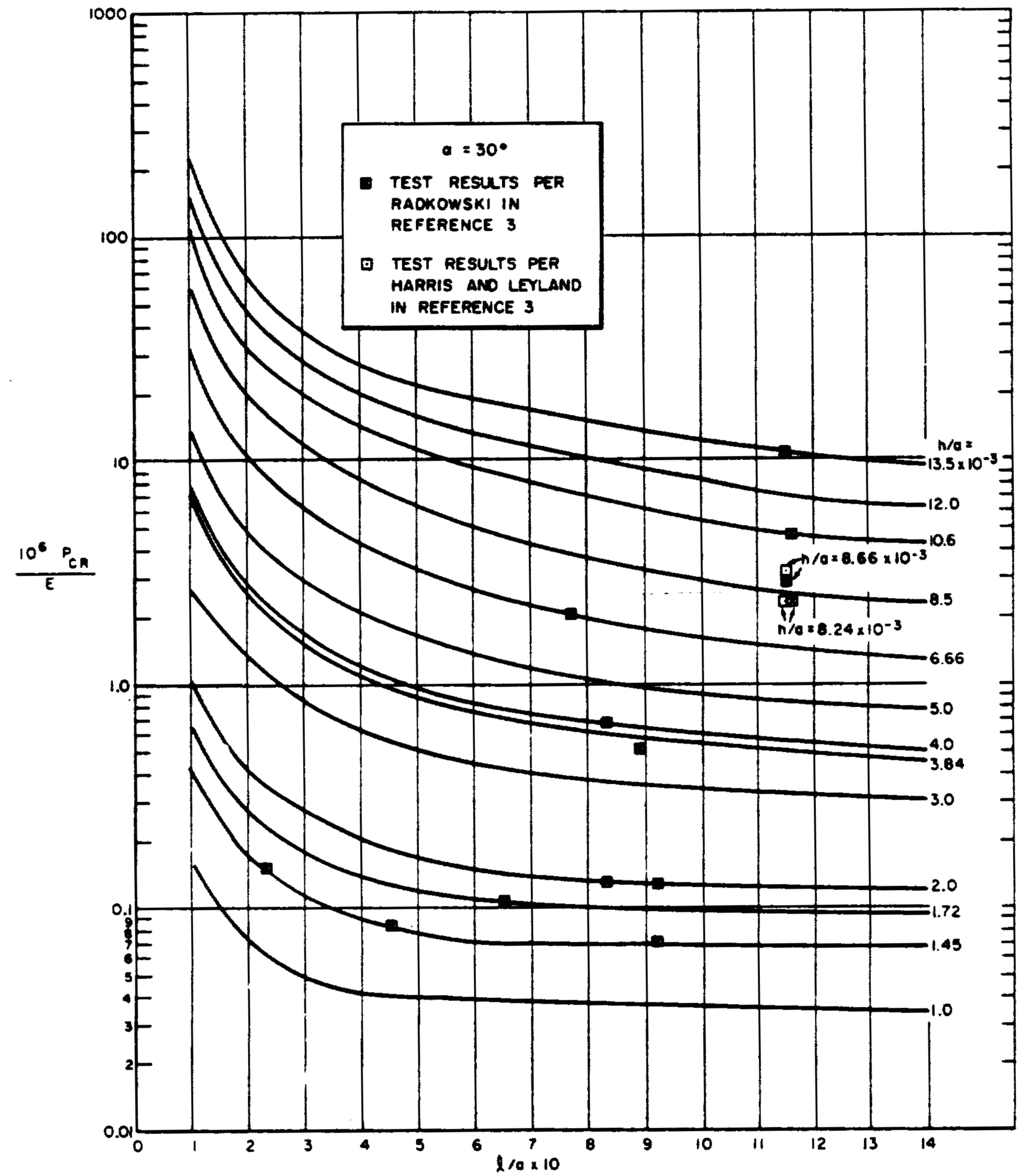

61-2622

Figure 2. - Instability of conical shells subjected to hydrostatic pressure.

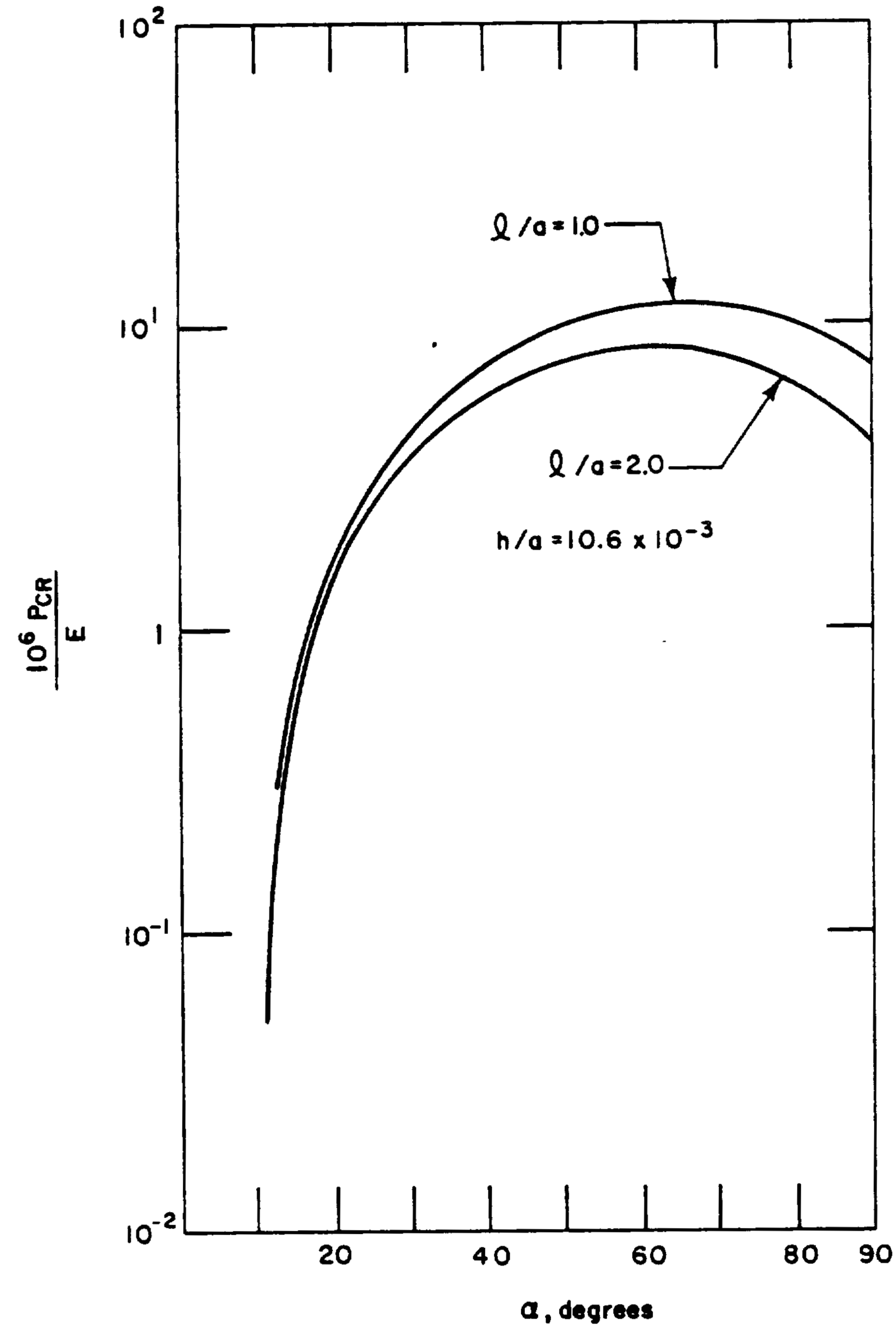

Figure 3. - Effect of cone angle on the buckling of conical shell subjected to hydrostatic pressure.

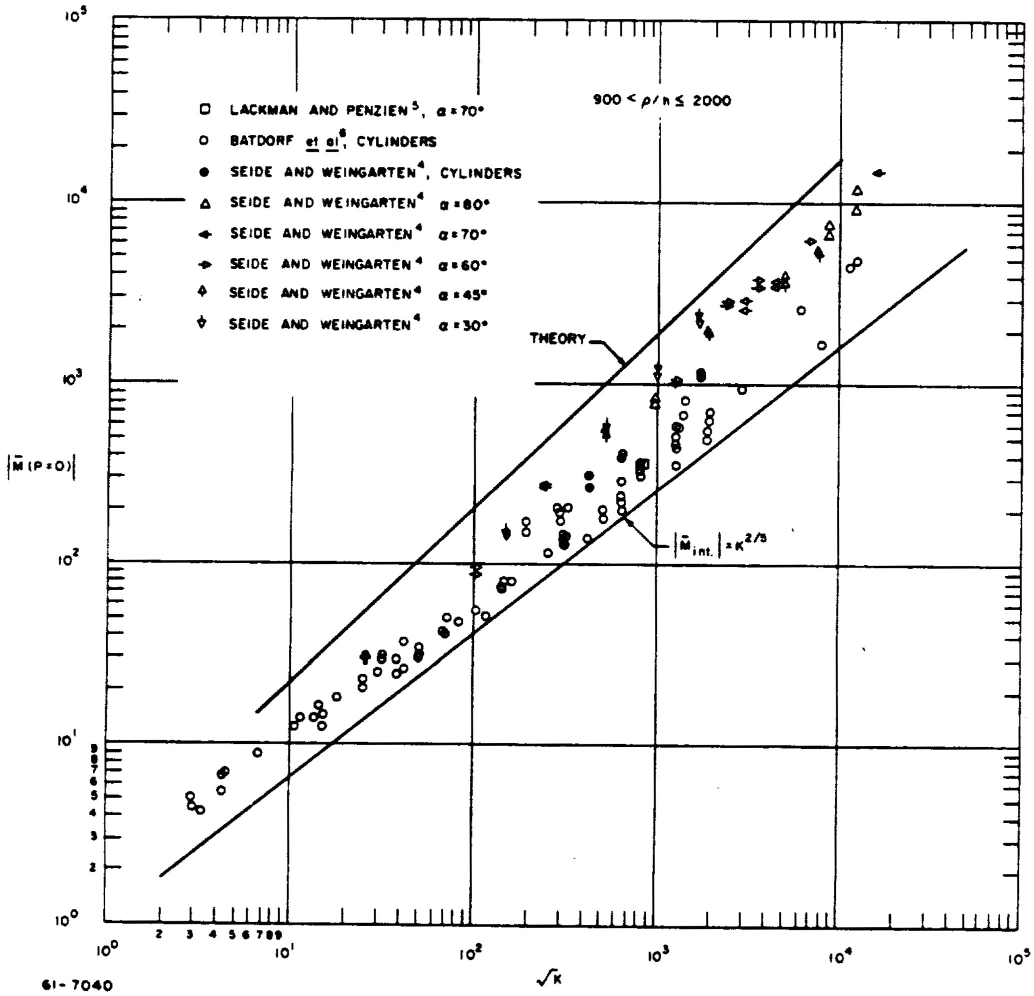

Figure 4. - Axial loading curves for thin single- and multi-layer conical and cylindrical shells.

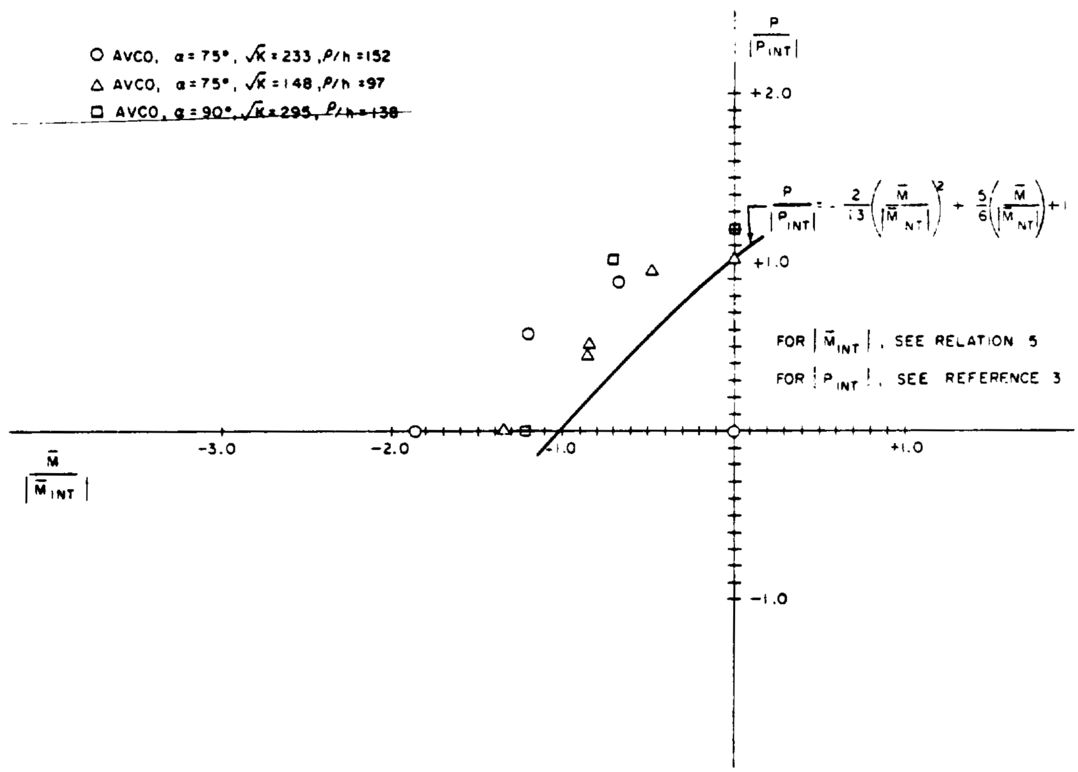

Figure 5. - Combined loading design curve for thin single- and multi-layer conical and cylindrical shells.

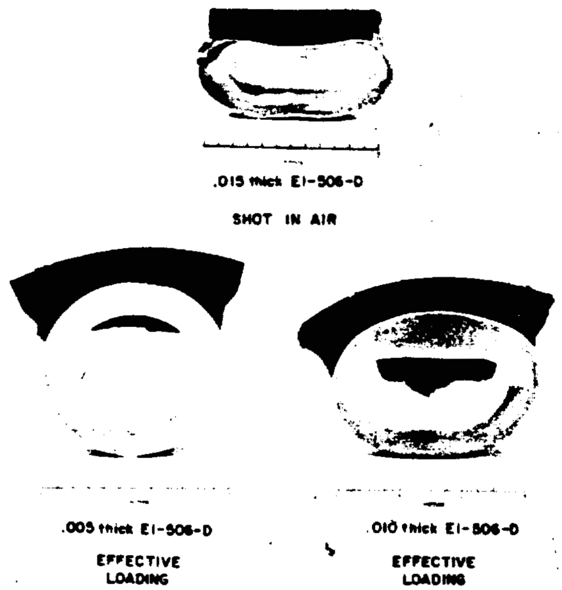

Figure 6.- Final configuration of magnesium cylinder series (courtesy S.R.I.).

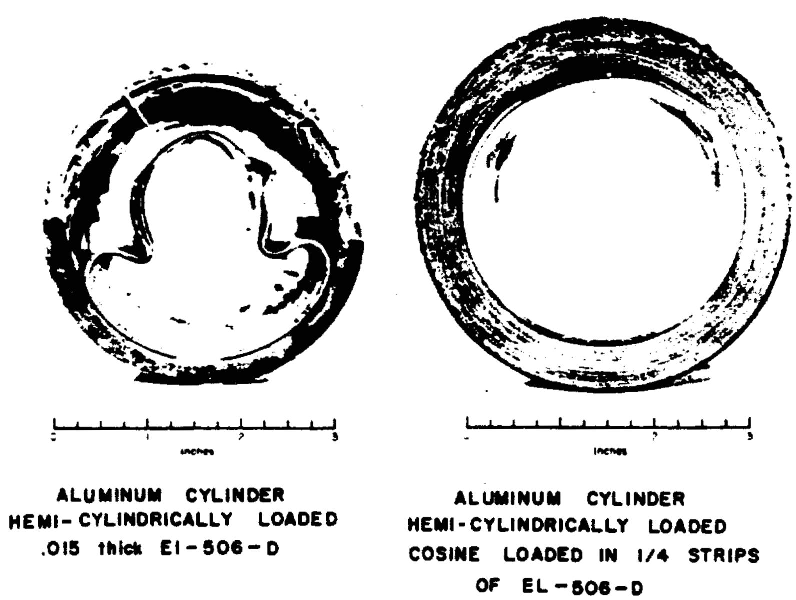

Figure 7.- Final configuration of cylinders with stiff outer layer after explosive test (courtesy S.R.I.).